



**HAL**  
open science

## Challenging development of storable particles for oral delivery of a physiological nitric oxide donor

Yi Zhou, Caroline Gaucher, Isabelle Fries, Mehmet-Akif Hobekkaya, Charlène Martin, Clément Leonard, Frantz Deschamps, Anne Sapin-Minet, Marianne Parent

### ► To cite this version:

Yi Zhou, Caroline Gaucher, Isabelle Fries, Mehmet-Akif Hobekkaya, Charlène Martin, et al.. Challenging development of storable particles for oral delivery of a physiological nitric oxide donor. Nitric Oxide: Biology and Chemistry, 2020, 104-105, pp.1-10. 10.1016/j.niox.2020.08.001 . hal-02922699

**HAL Id: hal-02922699**

**<https://hal.univ-lorraine.fr/hal-02922699v1>**

Submitted on 24 Aug 2022

**HAL** is a multi-disciplinary open access archive for the deposit and dissemination of scientific research documents, whether they are published or not. The documents may come from teaching and research institutions in France or abroad, or from public or private research centers.

L'archive ouverte pluridisciplinaire **HAL**, est destinée au dépôt et à la diffusion de documents scientifiques de niveau recherche, publiés ou non, émanant des établissements d'enseignement et de recherche français ou étrangers, des laboratoires publics ou privés.



Distributed under a Creative Commons Attribution - NonCommercial 4.0 International License

## **Challenging development of storable particles for oral delivery of a physiological nitric oxide donor**

**Yi ZHOU<sup>a</sup>, Caroline GAUCHER<sup>a</sup>, Isabelle FRIES<sup>a</sup>, Mehmet-Akif HOBEKKAYA<sup>a</sup>, Charlène MARTIN<sup>a</sup>, Clément LEONARD<sup>b</sup>, Frantz DESCHAMPS<sup>b</sup>, Anne SAPIN-MINET<sup>a</sup>, Marianne PARENT<sup>a,\*</sup>**

<sup>a</sup> Université de Lorraine, CITHEFOR, F-54000 Nancy, France

<sup>b</sup> StaniPharm, 5 rue Jacques Monod, BP 10, 54250 Champigneulle, France

\*Correspondence: [marianne.parent@univ-lorraine.fr](mailto:marianne.parent@univ-lorraine.fr), EA 3452 CITHEFOR, Campus Brabois Santé, 9 avenue de la Forêt de Haye - BP 20199, 54505 Vandoeuvre Les Nancy Cedex, Tel +33-3-7274-7307

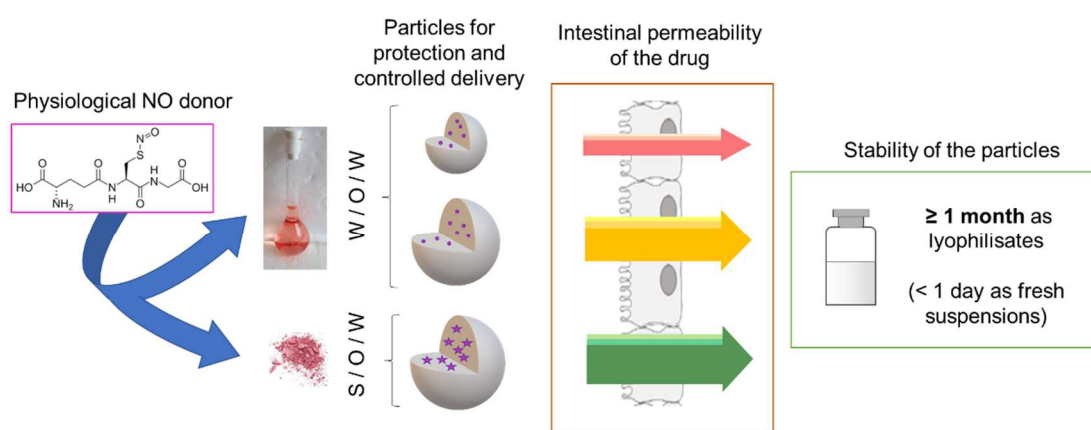
Mr Yi ZHOU was supported by a CSC (China Scholarship Council) funding.

The authors acknowledge support of EA 3452 CITHEFOR by the “Impact Biomolecules” project of the “Lorraine Université d’Excellence” (Investissements d’avenir – ANR).

These funding sources were not involved in study design, collection, analysis, interpretation of data, writing of the report nor in the decision to submit it for publication.

Declarations of interest: none

## Graphical Abstract:



## Abstract:

Nitric oxide (NO) deficiency is often associated with several acute and chronic diseases. NO donors and especially *S*-nitrosothiols such as *S*-nitrosoglutathione (GSNO) have been identified as promising therapeutic agents. Although their permeability through the intestinal barrier have recently be proved, suitable drug delivery systems have to be designed for their oral administration. This is especially challenging due to the physico-chemical features of these drugs: high hydrophilicity and high lability. In this paper, three types of particles were prepared with an Eudragit polymer: nanoparticles and microparticles obtained with a water-in-oil-in-water emulsion/evaporation process *versus* microparticles obtained with a solid-in-oil-in-water emulsion/evaporation process. They had a similar encapsulation efficiency (around 30%), and could be freeze-dried then be stored at least one month without modification of their critical attributes (size and GSNO content). However, microparticles had a slightly slower *in vitro* release of GSNO than nanoparticles, and were able to boost by a factor of two the drug intestinal permeability (Caco-2 model). Altogether, this study brings new data about GSNO intestinal permeability and three ready-to-use formulations suitable for further preclinical studies with oral administration.

**Keywords:** nitric oxide, *S*-nitrosoglutathione, nanoparticles, microparticles, oral delivery

## Highlights:

- GSNO is a promising drug, but challenging to formulate (hydrophilicity, lability)
- Nano and microparticles suitable for GSNO oral delivery were produced and compared
- Their critical attributes were maintained after freeze-drying and stable upon storage
- They improved the drug permeability through a Caco-2 model of intestinal barrier

## 1 1. Introduction

2 Nitric oxide (NO) is a radical messenger with a variety of physiological roles, *e.g.* control of vascular  
3 tone, neurotransmission at both central and peripheral levels, mediation of immune response,  
4 wound healing, tissue regeneration and anti-cancer defense [1]. As a result of these pleiotropic  
5 actions, many pathological conditions are accompanied by a NO deficiency (*e.g.* atherosclerosis,  
6 pulmonary hypertension, thrombosis, ischemia... [2-5]). As these conditions are becoming  
7 increasingly frequent in the population with ageing, a treatment able to restore the physiological NO  
8 levels would represent a major therapeutic advance for a growing number of patients.

9 NO itself cannot be used directly in many cases because of its very short half-life (< 1 s) [6].  
10 Moreover, its gaseous nature makes it difficult to store, to transport and to administer. In this  
11 context, NO donors have been developed over the past decades, including organic nitrates [7-8],  
12 nitrosamines [9], metal-NO complexes [10], diazenium-diolates (NONOates, [11]) and S-nitrosothiols  
13 (RSNO, [12-13]). As RSNO are the physiologic forms of NO transport and storage in our body, they are  
14 considered as “hot candidates” with no efficacy nor toxicity concerns. In particular, S-  
15 nitrosoglutathione (GSNO) has gained a lot of attention in preclinical and clinical trials for different  
16 biomedical applications [14-15]. GSNO is a physiological low-molecular-weight RSNO, with  
17 arterioselective vasodilating and antiplatelet effects. Additionally, the NO moiety in GSNO is grafted  
18 to glutathione (GSH), which is the main redox buffer with antioxidant properties in our cells. Thus,  
19 GSNO will release both NO and GSH: this could be beneficial as NO deficiency is generally associated  
20 to oxidative stress in many conditions. However, pharmacokinetics data are drastically limited by the  
21 fact that GSNO is a very hydrophilic (clogP = - 2.7) and labile active drug, highly reactive to its  
22 environment. GSNO is rapidly degraded or metabolized by several (*e.g.* protein disulfide isomerases  
23 [16], thioredoxins [17], GSNO reductase [18], gamma-glutamyl transpeptidase [19]). RSNO  
24 metabolism leads to the formation of multiple NO-derived species (NO<sub>x</sub>, including nitrite and nitrate  
25 ions), therefore difficult to follow throughout the entire organism. Only few studies have attempted  
26 to define RSNO pharmacokinetic parameters, especially after oral administration, as this require  
27 technically demanding methods (radioisotope tracking of NO [20-21]). Furthermore, little is known  
28 on the crossing of the intestinal barrier by RSNO. Bonetti et al. [22] revealed the ability of 3 RSNO  
29 (including GSNO) to cross the intestinal barrier (Caco-2 model) with a medium apparent permeability  
30 rate, using a passive mode. As the therapeutic effects of NO depend not only on the location of  
31 production/release, but also on the rate and quantity of available NO, it is a real pharmaceutical  
32 challenge to propose a formulation of GSNO able to protect and to deliver it properly. As already  
33 mentioned, to the great distress of formulators, GSNO is very sensitive: to light, oxygen, heat, pH  
34 changes, or presence of thiols or metallic ions even at low concentrations. As a drug, GSNO can be  
35 stored only as powder, at -20°C, protected from light and under an inert atmosphere. Precautions  
36 (ultrapure water, light protection) have to be taken to prepare GSNO solutions, which should be  
37 discarded after few hours. These characteristics make it very challenging and raise many hurdles to  
38 develop GSNO formulations adapted to oral delivery, the most attractive route of administration to  
39 manage patients in the context of chronic diseases.

40 Among the few examples in the literature, conjugation of GSNO to diblock polymers was proposed  
41 [23] as well as direct encapsulation of GSNO into various hydrophilic (alginate, chitosan...) or  
42 hydrophobic polymeric matrices [24-29]. Hydrophilic polymers have generally less standardized  
43 characteristics because of their natural origin. Their hydrophilic nature is favorable for GSNO  
44 encapsulation, but the resulting loose hydrogels might lead to a fast drug release. Among  
45 hydrophobic polymers, the Eudragit ones are especially interesting, as they are mucoadhesive  
46 excipients already approved for human oral administration.

47 Wu et al. [30] used Eudragit RLPO, commonly used for tablet coating, to prepare nanoparticles which  
48 were incorporated into an alginate/chitosan matrix to enhance GSNO loading and release profile  
49 [31]. The resulting composite microparticles generated a NO store in rat aorta after a single oral  
50 administration [32]. Despite of these very interesting results, the preclinical development of these  
51 composites formulations is hindered by several points. First, the multi-step preparation and the  
52 adequate characterization are too time-consuming. Second, these formulations are not stable and  
53 should be used immediately after preparation (no possibility to be sent to other labs to be tested in  
54 preclinical models).

55 Following these precedents, the aims of this work were to: (i) propose a new drug delivery system  
56 that enables GSNO stabilization and controlled release; (ii) provide information on GSNO intestinal  
57 absorption from these developed delivery systems.

58 To overcome these barriers, GSNO-loaded Eudragit RLPO particles adapted for oral delivery were  
59 prepared, with a reasonably simple protocol, at least similar encapsulation efficiency and release  
60 profile than the previously described particles, and with a sufficient stability to be stored and/or sent  
61 before use. According to the hydrophilic nature of the drug, microparticles (MP) were prepared by  
62 double emulsion/solvent evaporation, either with a water-in-oil-in water (W/O/W) process (GSNO-  
63 MPW) or a solid-in-oil-in-water (S/O/W) process (GSNO-MPS). They were compared to nanoparticles  
64 obtained with a W/O/W process (GSNO-NP) in terms of size, encapsulation efficiency and *in vitro*  
65 release. Moreover, to get particles in a stable solid state, a lyophilization process was applied.  
66 Potential modifications of critical product attributes (GSNO content and particle size) were assessed  
67 immediately after lyophilization and during refrigerated storage. Afterwards, the cytocompatibility of  
68 the particles was evaluated on Caco-2 cells. Finally, intestinal permeability of NO<sub>x</sub> species was  
69 evaluated using an *in vitro* model of intestinal barrier.

70

## 71 **2. Material and methods**

72 All solutions were prepared with ultrapure deionized water (> 18.2 MΩ.cm). GSNO powder was  
73 synthesized, purified and stored as previously described [31]. Eudragit® RLPO was a gift from Evonik  
74 industries (Germany). HgCl<sub>2</sub> was purchased from Prolabo (Switzerland), NaNO<sub>2</sub> from Merck  
75 (Germany), NaOH from VWR Chemicals (Czech Republic), methanol from Carlo Erba Reagents  
76 (France). All other reagents were obtained from Sigma–Aldrich (France).

### 77 **2.1. GSNO powder synthesis**

78 GSNO powder was synthesized, purified and stored as previously described [33]. Briefly, sodium  
79 nitrite and reduced glutathione (GSH), equivalent amount, were incubated under acidic condition  
80 (0.626 M HCl). The solid form of GSNO was obtained by cold acetone precipitation, then washed,  
81 dried under vacuum and stored at -20°C under inert dinitrogen atmosphere. GSNO purity > 95% is  
82 required for batch release (see [33] for details about control).

### 83 **2.2 Quantification of GSNO, nitrite ions and nitrate ions**

84 Nitrite ions and GSNO were quantified using a colorimetric (Griess and Griess-Saville reactions) or a  
85 fluorimetric method (diaminonaphthalen (DAN) and DAN-Hg<sup>2+</sup>) with standard curves of sodium  
86 nitrite and GSNO, respectively. Briefly, N<sub>2</sub>O<sub>3</sub> generated from acidified nitrite ions reacts with Griess  
87 reagent (Sulfanilamide and N-(1-naphthyl)ethylenediamine) or DAN in the presence (for GSNO) or  
88 absence (for nitrite ions) of HgCl<sub>2</sub> producing a diazonium salt or 2,3-naphthotriazole that either  
89 absorbs at 540 nm or emits fluorescence at 415 nm after excitation at 375 nm (JASCO FP-8300,

90 France). GSNO concentration was obtained by subtracting Griess to Griess-Saville quantification or  
 91 DAN to DAN-Hg<sup>2+</sup> quantification. Nitrate ions quantification (using a standard curve of sodium  
 92 nitrate) included a reduction step of nitrate in nitrite ions using a nitrate reductase and its cofactors  
 93 before the addition of DAN reagent (fluorometric kit nitrite/nitrate Cayman Chemical Ref. 780051,  
 94 USA). Nitrate concentration was obtained by subtracting DAN-Hg<sup>2+</sup> quantification to nitrate  
 95 quantification using nitrate reductase.

## 96 2.3. Preparation and lyophilization of GSNO-loaded particles

### 97 2.3.1. Preparation of GSNO-loaded nanoparticles and microparticles

98 GSNO-loaded nanoparticles (GSNO-NP) were prepared by a water-in-oil-in-water (W/O/W)  
 99 emulsion/solvent evaporation technique [30]. Briefly, 500  $\mu$ L of 0.1% (w/v) Kolliphor P188 solution  
 100 containing 10 mg of GSNO was emulsified by sonication for 60 s (11 W, 100% amplitude, Vibra cell™  
 101 72434, France) in 5 mL of methylene chloride containing 500 mg of Eudragit, over an ice bath. The  
 102 resulting primary emulsion was then poured in 19.5 mL of 0.1% (w/v) Kolliphor P188 solution with  
 103 ultrasonication (30 W, amplitude maximum, Vibra cell™ 75022, France) for 30 s, to get the W/O/W  
 104 emulsion. The final GSNO-NP suspension was obtained after 10 min of solvent evaporation.

105 GSNO-loaded microparticles were prepared by W/O/W process (GSNO-MPW) or by S/O/W process  
 106 (GSNO-MPS). GSNO-MPW preparation followed the same process as GSNO-NP, except for the second  
 107 emulsification, which was performed with a vortex (VV3, VWR, USA) at maximum speed for 60 s,  
 108 rather than with ultrasonication. The whole process was conducted at controlled temperature ( $24 \pm$   
 109  $0.5$  °C). GSNO-MPS were prepared as GSNO-MPW, except that 10 mg of GSNO powder (sieved at  
 110  $40$   $\mu$ m) were directly suspended in the Eudragit/DCM solution. Attempts to reduce the size of GSNO  
 111 powder grain were made with supercritical fluid technology (see Table 1).

112 **Table 1. Conditions used in supercritical trials to decrease the size of GSNO powder grains.** Gaseous  
 113 antisolvent (GAS) and supercritical antisolvent (SAS) processes rely on the use of the supercritical CO<sub>2</sub>  
 114 as an anti-solvent. The crystallization of GSNO is induced by the mass transfer of the solvent (DMSO)  
 115 in the supercritical phase.

Treatment	Crystallization conditions	Drying conditions
<b>GAS</b>	Crystallization pressure: 300 bar Crystallization temperature: 40°C GSNO 1% wt in DMSO 10.9 g of solution injected CO <sub>2</sub> pressurization: 150 bar/min Equilibrium: agitation 54 rpm 10 min before drying 20 mL autoclave	300 bar/40°C CO <sub>2</sub> flow rate: 0.6 kg/h Duration: 3 h
<b>SAS</b> (1 <sup>st</sup> trial)	Crystallization pressure: 300 bar Crystallization temperature: 40°C GSNO 1% wt in DMSO 15.8 g of solution injected Molar CO <sub>2</sub> fraction: 0.984 2.2 kg <sub>CO2</sub> /h – 1.0 g <sub>sol</sub> /min Coaxial nozzle (100 $\mu$ m i.d.) 300 mL autoclave	300 bar/40°C CO <sub>2</sub> flow rate: 1.0 kg/h Duration: 2 h 30

---

	Crystallization pressure: 160 bar	
	Crystallization temperature: 40°C	
	GSNO 1% wt in DMSO	
<b>SAS</b>	22.1 g of solution injected	160 bar/40°C
(2 <sup>nd</sup> trial)	Molar CO <sub>2</sub> fraction: 0.971	CO <sub>2</sub> flow rate: 1.1 kg/h
	1.1 kg <sub>CO2</sub> /h – 1.0 g <sub>sol</sub> /min)	Duration: 3 h
	Coaxial nozzle (130 μm i.d.)	
	300 mL autoclave	

---

116

### 117 2.3.2. Lyophilization of GSNO-loaded particles

118 After particles preparation, the suspensions were centrifuged (42,000 g, 4°C, 30 min for NP or 10 min  
 119 for MP) and the pellets were re-suspended in 10 mL of 10% (w/v) sucrose solution. The re-  
 120 suspensions were frozen at -80°C for 15 h ± 1 h then lyophilized for 24 h ± 1 h (FreeZone6  
 121 LABCONCO USA, setups: condenser at -50°C and pressure at 0.04 mbar). A preliminary study was  
 122 conducted to optimize the lyophilization of GSNO-NP and to select the best and lowest-cost  
 123 conditions such as -80 °C freezing of the particles (instead of liquid nitrogen) and using sucrose as  
 124 protectant (instead of trehalose, and no mannitol). The residual water content in the lyophilizate was  
 125 immediately tested after freeze-drying using a Karl-Fischer apparatus (756 KF coulometer, France).  
 126 All powders were placed under nitrogen and stored at 4°C protected from light.

127

### 128 2.4. Physicochemical characterization of particles

129 The hydrodynamic diameter, polydispersity index (PDI) and zeta-potential of the GSNO-NP were  
 130 measured in triplicate in 1 mM NaCl by dynamic light scattering (Zetasizer Nano ZS, Malvern  
 131 Instrument, France). All measurements were performed at 25°C after 30 s of equilibration with an  
 132 angle detection of 173° backscatter.

133 The size of GSNO-MP was also measured in triplicate in 0.001 M NaCl by a Mastersizer (hydro 2000  
 134 SM, Malvern Instruments, France). Span was calculated as follows:

$$135 \text{ Span} = (Dv90 - Dv10) / Dv50$$

136 where Dv10, Dv50, Dv90 are values of size below which 10%, 50% or 90% of the particles are  
 137 contained.

138 The surface morphology of the particles was investigated by scanning electron microscopy (SEM,  
 139 Hitachi S4800, Japan, accelerating voltage 1 kV). Briefly, fresh suspension of GSNO-NP was diluted  
 140 10<sup>6</sup>-fold. Then, a drop was deposited and dried overnight at room temperature, and flash carbon  
 141 coated (4 s). In the case of GSNO-MP, lyophilizates were observed after carbon coating.

142

### 143 2.5. Determination of GSNO encapsulation efficiency (direct method)

144 The encapsulation efficiency (EE) was determined by quantifying the GSNO contained inside the  
 145 particles. After particles centrifugation (42,000 g, 30 min for NP, 10 min for MP), the pellets were  
 146 collected and destroyed by methylene chloride. GSNO was then extracted with phosphate buffer  
 147 saline (0.148 M PBS, pH=7.4) (ratio methylene chloride/PBS 1:10) using high speed shaking  
 148 (2,000 rpm, Heidolph Vibramax 110, Germany). After centrifugation (2,500 g for 10 min), GSNO and  
 149 nitrite ions were quantified in the supernatant using Griess-Saville and Griess reactions. GSNO

150 concentration was deduced by subtracting Griess quantification to Griess-Saville quantification.  
151 Total recovery of GSNO during the extraction process has been verified and potential matrix effect  
152 with polymer residues have been ruled out in preliminary experiments. The encapsulation efficiency  
153 was assessed immediately after particles preparation and calculated according to:

$$154 \quad EE = (m_e / m_i) * 100\%$$

155 Where EE is encapsulation efficiency (%),  $m_e$  is the mass of drug entrapped in particles, and  $m_i$  is the  
156 mass of initial drug. The determination of GSNO content inside the particles after lyophilization and  
157 during storage was performed using the same protocol (the residual water content of the  
158 lyophilizates was considered in the calculations).

159

## 160 **2.6. Stability of particles before and after lyophilization**

161 After preparation, fresh suspensions of particles were centrifuged (42,000 g, 4°C, NP for 30 min and  
162 MP for 10 min). The pellets were re-suspended in 1 mL water and stored at 5±3°C protected from  
163 light. After 1, 2, 3, or 4 days, size and GSNO and potential nitrite content of separated aliquots were  
164 measured as previously described.

165 After lyophilization, the particle powders were stored at 5±3°C under nitrogen and protected from  
166 light. After 1, 2, 3, 4, 5, 8 and 12 weeks, size and GSNO content of separated aliquots were checked  
167 as previously described and compared to the values obtained immediately after lyophilization.

168

## 169 **2.7. Kinetics of GSNO release**

170 Immediately after preparation, 1 mL of fresh particles suspensions were centrifuged (42,000 g, 4°C,  
171 30 min for NP and 10 min for MP). The pellets were suspended in 1 mL of 0.148 M PBS (pH 7.4) and  
172 transferred into dialysis cellulose membrane (average flat width 10 mm (0.4 in), cut-off 14,000 Da).  
173 The membrane was immersed in 200 mL PBS at 37°C protected from light with magnetic agitation at  
174 200 rpm. The GSNO and nitrite ions released in the medium were quantified using the DAN and DAN-  
175 Hg<sup>2+</sup> methods at different time intervals (every 30 min during two hours and every hour from two to  
176 six hours) [30].

177

## 178 **2.8. Cytocompatibility of particles**

179 Intestinal Caco-2 cells (ATCC® HTB-37™) were grown in complete medium consisting of Eagle's  
180 Minimum Essential Medium supplemented with 10% (v/v) fetal bovine serum (FBS), 4 mM of  
181 glutamine, 100 U/mL of penicillin, 100 U/mL of streptomycin, 1% (v/v) of non-essential amino acids.  
182 Cells were cultivated at 37°C under 5% CO<sub>2</sub> (v/v) in a humidified incubator. Cells were then seeded in  
183 96-well plates at 10<sup>5</sup> cells/well. After 24 h, cells were exposed to free GSNO (from 25 µM to 2500  
184 µM) or to lyophilizate particles (3 batches, in duplicate, at equivalent GSNO concentrations from 25  
185 µM to 2500 µM) for 24 h in complete medium. After incubation, cytocompatibility was checked by  
186 the 3-(4,5-dimethylthiazol-2-yl)-2,5-diphenyltetrazolium bromide (MTT) method [22]. The  
187 absorbance was read at 570 nm with a reference at 630 nm using EL 800-microplate reader (Bio-TEK  
188 Instrument, France). Metabolic activity in the presence of treatments was compared to the control  
189 condition, i.e. medium alone (as 100%).

190



## 191 **2.9. Intestinal Permeability**

192 Caco-2 cells were seeded at  $2 \times 10^6$  cell/cm<sup>2</sup> on cell culture inserts (Transwell®, Corning, USA) with  
193 0.4 μm pore size disposed in a 12-wells plate. Complete medium was replaced every two days during  
194 the first week and every day during the second week. The intestinal barrier was validated when the  
195 differentiated cell monolayer was obtained after 14-15 days of culture with a transepithelial  
196 electrical resistance (TEER) value > 500 Ω.cm<sup>2</sup>. Intestinal permeability of the 3 different lyophilized  
197 particles (GSNO concentration 100 μM in all cases, 3 batches, in triplicate) was compared to free  
198 GSNO in HBSS containing Ca<sup>2+</sup> and Mg<sup>2+</sup> (HBSS+). Two controls of permeability and integrity of the  
199 intestinal barrier model using HBSS+ and HBSS without Ca<sup>2+</sup> and Mg<sup>2+</sup> (HBSS-) were performed. After  
200 1 h of incubation, the amounts of NOx species (i.e. RSNO + nitrite ions + nitrate ions) were quantified  
201 using DAN-Hg<sup>2+</sup>, DAN methods with or without nitrate reductase, in the apical compartment both  
202 free in the medium and inside the particles, and in the basolateral compartment. A TEER value higher  
203 than 300 Ω.cm<sup>2</sup> and a fluorescein permeability lower than 5% at the end of the test validated the  
204 integrity of the intestinal monolayer [22].

205 The apparent permeability coefficients (P<sub>app</sub>) were calculated as follows:

$$206 P_{app} = (dQ/dt) \times (1/(A \times C_0))$$

207 Where dQ/dt (mol.s<sup>-1</sup>) refers to the permeability rate (mol) of RSNO or NOx in the basolateral  
208 compartment at the time of quantification, A (cm<sup>2</sup>) to membrane diffusion area, and C<sub>0</sub> (mol.mL<sup>-1</sup>) to  
209 the initial concentration in the apical compartment.

210 The recovery rate of NOx species (mass balance of GSNO) was checked by comparing the amount of  
211 NOx species quantified in the different compartments (apical, basolateral, in the particles) with the  
212 initial amount of GSNO deposited.

213

## 214 **2.10. Statistical analysis**

215 All the results are shown as either mean ± standard deviation (sd, for characterization) or mean ±  
216 standard error of mean (sem, for cells results). In all cases, three independent batches (preparation  
217 and lyophilization) were used.

218 The one-way ANOVA or two-way ANOVA (Dunnett's multiple comparisons test or Tukey's multiple  
219 comparisons test) were used for the analysis of particles stability, release and Caco-2 cells  
220 experiments. p < 0.05 was considered as significantly different. Statistical analyses were performed  
221 using the GraphPad Prism software (GraphPad Software, USA).

222

## 223 **3. Results and discussion**

224 Currently, pharmacokinetic data of the orally administered GSNO are lacking while its  
225 pharmacodynamic effects are well documented and indicate a great therapeutic potential. For  
226 example, a recent literature review from Liu et al. [15] highlighted the results obtained with GSNO in  
227 clinical trials and preclinical models of stroke: repeated oral administration is used in several of the  
228 preclinical studies with promising cerebro-protective or regenerative effects against ischemic lesions,  
229 without deciphering the drug transport across the intestinal nor the haemato-encephalic barriers.  
230 This absence of information limits the use of GSNO as a therapeutic drug. A pioneer work has been  
231 done by Wu et al. [31], whose composite particles promoted GSNO intestinal permeation and led to  
232 the formation of releasable NO store in rat aorta 17 h after a single oral administration. However, a

233 lot of work remains to be done to implement data and identify the "best" way to present the drug  
234 (*i.e.* drug delivery system) to the intestinal barrier and how it will impact the drug permeability.  
235

### 236 **3.1. Particles size and encapsulation efficiency**

237 The double emulsion/solvent evaporation method is generally suitable for hydrophilic drugs and was  
238 previously successfully applied for GSNO encapsulation into Eudragit RLPO [30]. The process applied  
239 with two successive ultrasonic emulsifications and methylene chloride evaporation led to a  
240 submicronic formulation. However, the encapsulation was still limited and no sustained release was  
241 described. The optimization of this formulation process is the challenge of our present study. Starting  
242 from the same raw materials (and the same drug/polymer ratio), the initial W/O/W protocol was  
243 modified in two ways. On the one hand, the second emulsion step was modified to produce  
244 microparticles (GSNO-MPW) instead of nanoparticles (GSNO-NP), as the lower energy emulsification  
245 might protect GSNO from degradation. Additionally, the bigger size of the emulsion droplets and  
246 resulting particles might both hinder drug leakage during particles preparation and slow down its  
247 release from hardened particles [34]. On the second hand, the S/O/W protocol was tested (GSNO-  
248 MPS), using GSNO powder instead of GSNO solution in the first emulsion. In comparison to W/O/W  
249 processes, S/O/W methods generally improve encapsulation efficiency of hydrophilic or sensitive  
250 drugs and can also lead to better release profiles [35-37].

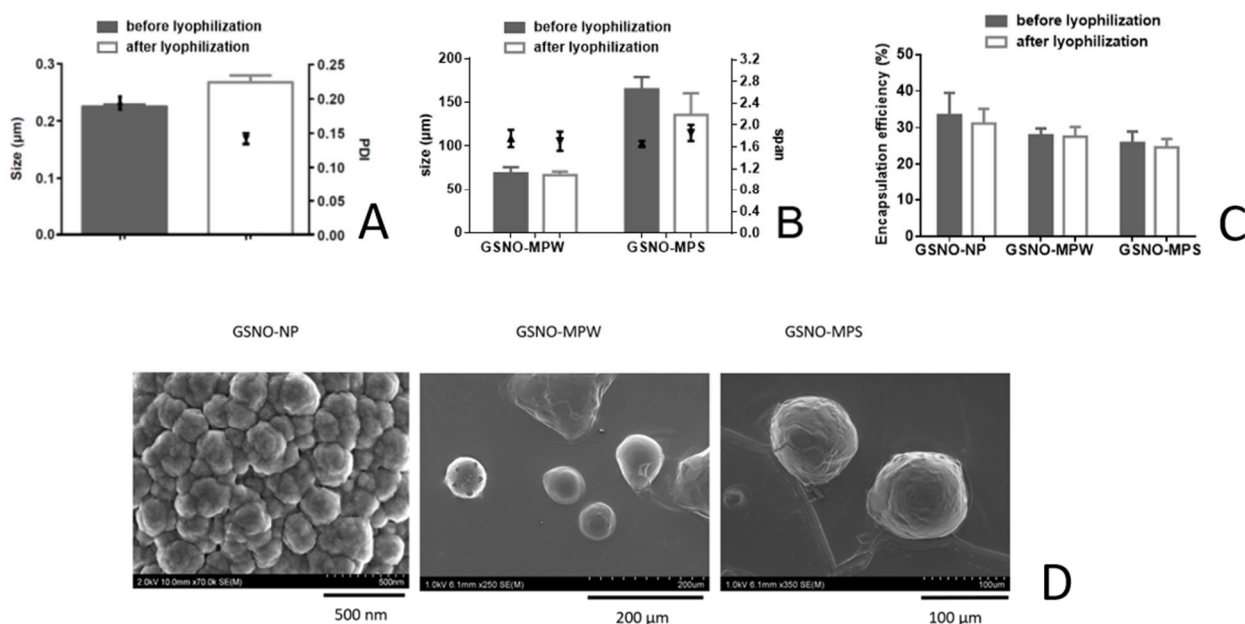
251 In our case, particles size was indeed increased, from  $0.225 \pm 0.003 \mu\text{m}$  for GSNO-NP to  $69 \pm 7 \mu\text{m}$  for  
252 GSNO-MPW and  $165 \pm 14 \mu\text{m}$  for GSNO-MPS. However, there was no improvement in the  
253 encapsulation efficiency ( $28 \pm 2\%$  for GSNO-MPS,  $26 \pm 3\%$  for GSNO-MPW, versus  $33 \pm 6\%$  for GSNO-  
254 NP), corresponding to a drug loading around 0.7% (w drug/w polymer). In all cases, the amount of  
255 nitrite ions was negligible ( $< \text{limit of quantitation } 0.5 \mu\text{M}$ ), meaning that the formulation process is  
256 suitable for this fragile drug, and that the mild encapsulation efficiency of GSNO is more likely caused  
257 by its low entrapment into the polymeric matrices rather than by its degradation.  
258

259 In the first step of the S/O/W method, the solid drug is dispersed into an organic solvent. A smaller  
260 size of the grain powder facilitates the homogeneous dispersion of the drug, thus improving its final  
261 encapsulation [38-39]. Grain size reduction is generally achieved with conventional grinding  
262 techniques, but the sensitivity of GSNO to thermal degradation, requires rather innovative  
263 supercritical fluid processes [40]. At first, a supercritical antisolvent (SAS 1<sup>st</sup> trial Table 1) process  
264 using DMSO was used. However, it led to a non-acceptable degradation of the drug ( $> 70\%$  loss). So,  
265 at second, a gaseous anti-solvent (GAS) process was selected, which failed to obtain any solid  
266 product, probably because of the too high solubility of GSNO in the  $\text{CO}_2/\text{DMSO}$  mixture, and a too  
267 high fraction of DMSO. Finally, the SAS process adapted with milder conditions (2<sup>d</sup> trial) led to a pink  
268 powder (yield 72%), with more than 80% purity. However, this GSNO powder was too hygroscopic  
269 and turned into a sticky product impossible to characterize. This could be due either to a high  
270 residual content of DMSO in the powder and/or to the specific features of GSNO, amplified by the  
271 higher surface area (reduction of powder particles size with the process). As a result, we used directly  
272 the raw GSNO powder in our experiments and dichloromethane as traditional solvent for the 3  
273 formulations tested (GSNO-NP, -MPW, -MPS) to compare GSNO intestine absorption in order to  
274 conduct a pharmacokinetic approach.  
275

### 276 **3.2. Stability: fresh suspensions versus lyophilized particles**

277 According to the International Conference on Harmonization (ICH) guidelines (Q1A (R2)), a drug  
278 product should be evaluated in studies where "the storage conditions and the lengths of studies  
279 chosen should be sufficient to cover storage, shipment and subsequent use". For our studies, we  
280 choose to store our products at  $5 \pm 3^\circ\text{C}$ , as a compromise between the thermal fragility of GSNO and

281 an easier storage/shipment. Moreover, due to the very challenging development of GSNO stable  
 282 particles, we considered that a 10% (and not 5% as in ICH) change from the initial value will be  
 283 considered significant for the critical product attributes, *i.e.* size and GSNO content.  
 284 When stored as suspensions, the size of all particles remained stable during three days (not shown).  
 285 This can be explained by the electrostatic repulsion between particles allowed by positive charges  
 286 (quaternary ammonium groups) brought by Eudragit RLPO polymer (zeta potential of GSNO-NP at  
 287  $+38 \pm 1$  mV). However, particles GSNO content dropped to less than 90% of the initial value after one  
 288 day, and fell around 60% after two days (not shown) for all suspensions. These results are consistent  
 289 with those reported previously for GSNO-NP [30-31].  
 290 Lyophilization using 10% w/v sucrose as cryoprotectant was successfully implemented to stabilize the  
 291 three particles types (GSNO-NP, -MPW, -MPS) without modifying their critical attributes (Figure 1A,  
 292 B, and C). A cryoprotectant was imperative to retain the GSNO content of the particles (no  
 293 cryoprotectant = more than 50 % of GSNO lost during freeze-drying), but sucrose was as effective as  
 294 trehalose. SEM images show that the particles are roughly spherical, with a more or less smooth  
 295 surface and no visible pores at the surface (Figure 1D). It was not possible to observe freeze-dried  
 296 powder of GSNO-NP (instead, fresh particles were observed), because the sucrose included in the  
 297 lyophilizate generated structures in the same range of size than NP.



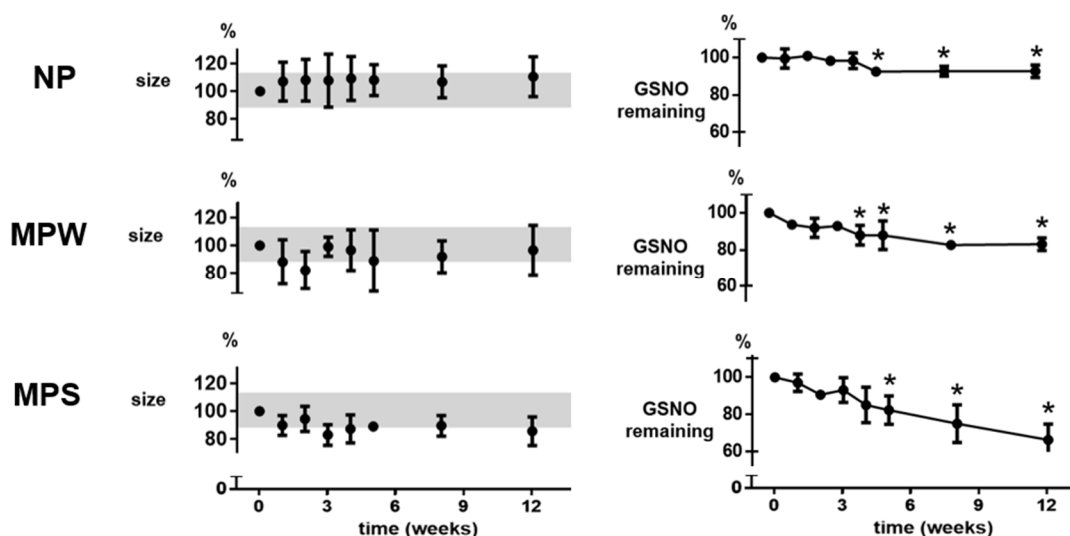
298  
 299 **Figure 1: Characterization of GSNO-loaded particles before and after lyophilization.** Size and  
 300 polydispersity index (PDI) of the GSNO-NP (A) as well as size and span of the GSNO-MP (B),  
 301 encapsulation efficiencies (C) are presented as mean  $\pm$  sd (n=3). Representative Scanning Electron  
 302 Microscopy images are also presented (D).

303  
 304 After lyophilization, size remain stable for the three types of particles during storage for the three  
 305 months of study (Figure 2). In contrast, GSNO content decreased significantly after four weeks of  
 306 storage for both kinds of microparticles, and more slowly for GSNO-NP (90% of initial content  
 307 remaining after three months). These results might be linked to the different residual water content  
 308 (w/w) of the lyophilizates, namely  $7 \pm 5\%$  for GSNO-NP,  $9 \pm 5\%$  for GSNO-MPW and  $26 \pm 11\%$  GSNO-  
 309 MPS. These values are rather high for freeze-dried formulations (usually  $< 2\%$ ). Either the freeze-

310 drying process was not sufficiently efficient, or the formulations have recaptured water before the  
 311 residual water content was measured (this was done as fast as possible, using dessicant to transport  
 312 the formulations, but it was not technically feasible to do it in a moisture-controlled environment).  
 313 This hygroscopic behavior echoes the one observed previously in the supercritical fluid experiments.  
 314 Further investigation of the freeze-drying process might be warranted.

315 However, more than 80% of the initial GSNO amount remained inside GSNO-MPS after one month  
 316 and inside GSNO-MPW after two months. This result offers a promising approach for oral delivery  
 317 system development.

318



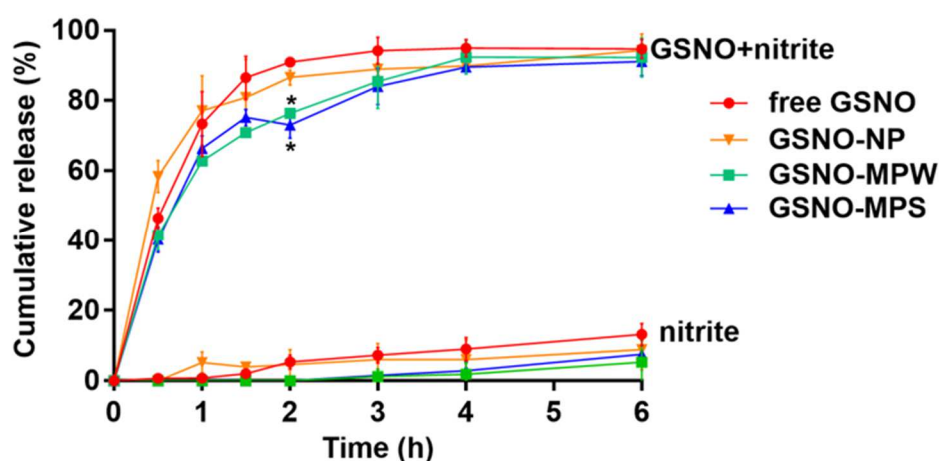
319

320 **Figure 2: Evolution of size and GSNO remaining for the GSNO-NP, GSNO-MPW and GSNO-MPS**  
 321 **particles stored at 4 °C under inert atmosphere after lyophilization.** Values measured immediately  
 322 after lyophilization are considered as 100%. Results are presented as mean ± sd (n = 3). The grey  
 323 areas delimit the sizes between 90% and 110% of the initial values. For GSNO remaining contents:  
 324 one-way ANOVA p < 0.05 for the three formulations (Dunnett's multiple comparisons test\* p < 0.05  
 325 versus week 0).

326

### 327 3.3. In vitro release

328 The kinetic release study was conducted under discriminating conditions (phosphate buffer), with no  
 329 ambition of *in vitro/vivo* correlation but to observe the ability of developed drug delivery systems to  
 330 protect and release GSNO in a controlled manner. The *in vitro* GSNO release profiles (Figure 3)  
 331 showed an initial burst in the first 1.5 h for all types of particles. At 2 h, the cumulative release from  
 332 microparticles was lower (around 70-75%) than for free GSNO and GSNO-NP (around 90% released).  
 333 Complete release was achieved after 6 h.



334

335 **Figure 3: In vitro drug release.** Results are presented as mean  $\pm$  sd (n = 3, free GSNO as control), two-  
 336 way ANOVA with  $p < 0.05$  for treatments, time and interaction (Tukey's multiple comparisons test: \*  $p$   
 337  $< 0.05$  versus free GSNO and GSNO-NP). The cumulative release is presented as total release ("GSNO  
 338 + nitrite", i.e. corresponding to the DAN-Hg<sup>2+</sup> assay, upper curves) or as nitrite ions ("nitrite", lower  
 339 curves, DAN assay).

340 In the recent literature, Lautner et al. [41] and Hlaing et al. [25] used S/O/W processes to encapsulate  
 341 RSNO into PLGA microparticles. With these polymers, they achieved higher drugs loadings  
 342 (respectively 12% for S-nitroso-N-acetylpenicillamine, SNAP, and 5% for GSNO) and sustained release  
 343 (several days). With our polymer especially adapted for oral administration, we obtained a 0.7% drug  
 344 loading, and a shorter release time, more suited for interaction with the gastrointestinal tract. These  
 345 results clearly highlight the challenge to encapsulate GSNO directly into hydrophobic particles  
 346 obtained by double emulsion/evaporation. Modifications of the drug (to increase its molecular  
 347 weight, for example using phytochelatins, natural polymers of GSNO analogues [42]) or of the  
 348 polymer (to graft GSNO directly on the polymer backbone) seem necessary to achieve high drug  
 349 loading/sustained release. An attractive alternative strategy mimicking the physiology could be to  
 350 encapsulate high molecular weight S-nitrosothiols, which will generate GSNO *in situ* by  
 351 transnitrosation of physiological GSH. Previous studies with encapsulation of S-nitroso-N-  
 352 acetylcysteine [43] and S-nitroso-captopril [44] proved the effectiveness of this transnitrosation  
 353 approach to elicit vasodilation or anti-infectious effects after parenteral or local administration,  
 354 respectively.

355 However, despite the lower encapsulation and duration of drug release with our Eudragit particles,  
 356 the release rate itself, around 150 pmol. mg<sup>-1</sup>.min<sup>-1</sup> for the first 1.5h, is in the range of previously  
 357 described PLGA systems encapsulating NO donors (e.g. from 40 pmol.mg<sup>-1</sup>.min<sup>-1</sup> with SNAP [41] to  
 358 400-800 pmol.mg<sup>-1</sup>.min<sup>-1</sup> with DETA NONOate [45]). So, the interaction of particles with a cell model  
 359 of intestinal barrier was evaluated.

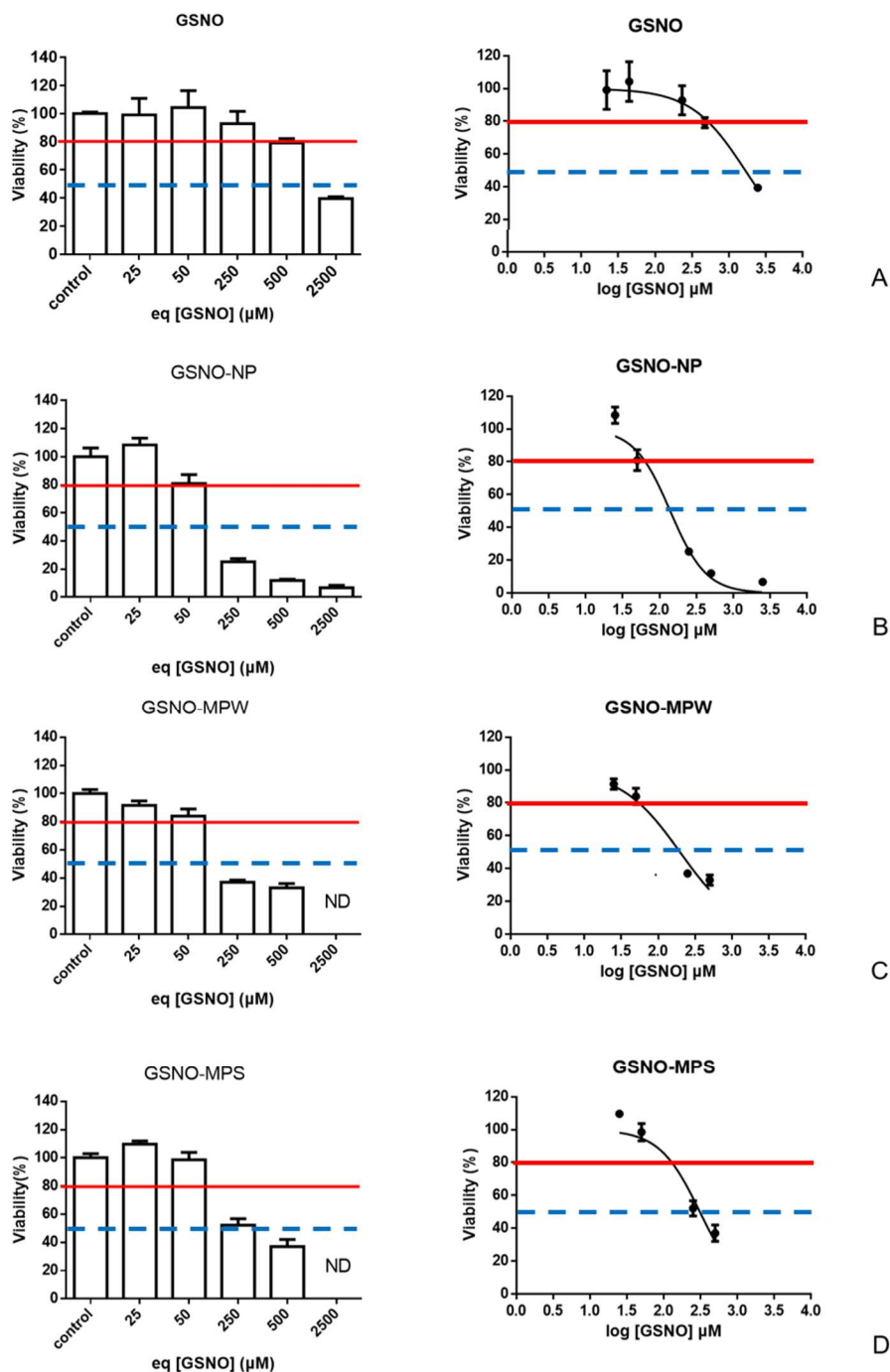
360

### 361 3.4. Cytocompatibility

362 The 24-h cytocompatibility of the three particle types and free GSNO decreased while increasing the  
 363 GSNO concentration (Figure 4). Concentrations tested in this study were deliberately far beyond the  
 364 ones needed for physiological effect of GSNO, in order to compare IC<sub>50</sub> values of free versus  
 365 encapsulated drug. The cell metabolic activity went below 80% for concentrations above 500  $\mu$ M for

366 free GSNO, and 50  $\mu\text{M}$  of eq [GSNO] for all particle types. The  $\text{IC}_{50}$  value of free GSNO ( $1718 \pm 1 \mu\text{M}$ )  
 367 decreased with its encapsulation in GSNO-MPS ( $310 \pm 1 \mu\text{M}$ ), GSNO-MPW ( $198 \pm 1 \mu\text{M}$ ) and GSNO-NP  
 368 ( $140 \pm 1 \mu\text{M}$ ).

369



370  
 371 **Figure 4: Cytocompatibility of Caco-2 cells after 24 h of incubation with GSNO (A), GSNO-NP (B),**  
 372 **GSNO-MPW (C), GSNO-MPS (D). Control condition = culture medium without fetal bovine serum.**  
 373 **Results are presented regarding GSNO loading, in equivalence of free GSNO from 25  $\mu\text{M}$  to 2500  $\mu\text{M}$ .**  
 374 **Results are shown as means  $\pm$  sem, n = 3 in duplicate. ND = not determined**  
 375

376 Eudragit RL (R for Retard) are poly(ethylacrylate, methyl methacrylate and methylammonio  
 377 ethylmethacrylate copolymers, bearing 8.8–12% quaternary ammonium groups. This material is  
 378 commonly employed for pH-independent coating of solid oral drug dosage forms. However, since it is  
 379 insoluble in water at physiological pH values and undergoes a certain degree of swelling, it may also  
 380 be suitable for the dispersion and controlled oral delivery of actives [46]. The cytocompatibility of  
 381 drug delivery based on this polymer is well documented. In this context, the results obtained were  
 382 not surprising. However, after oral administration, the concentration of 50  $\mu$ M (corresponding  
 383 roughly to 2.5 g/L of particles) should not be locally achieved in 24 h but distributed and spread  
 384 throughout the length of the intestine. In addition, it is important to note that the study conducted  
 385 here was voluntarily conducted on undifferentiated Caco-2 cells, known to be more sensitive than  
 386 the cells used for permeability studies (cultured for 15 days prior to the study) [47].

387

### 388 3.5. Intestinal permeability

389 The intestinal permeability of NO<sub>x</sub> species released from particles compared to free GSNO was  
 390 evaluated using an *in vitro* intestinal barrier model (Figure 6). Bonetti et al. [22] demonstrated  
 391 recently that free RSNO (GSNO, S-nitroso-N-acetylcysteine NACNO and SNAP), without drug delivery  
 392 systems, can cross this barrier (Caco-2 model) with a medium apparent permeability rate, using a  
 393 passive mode. In the present study, we wanted to explore the ability of Eudragit RL-based-drug  
 394 delivery systems to improve GSNO intestine permeability. To follow the future of NO through the  
 395 intestinal barrier, it is essential to follow the RSNO but also the degradation products (nitrite ions and  
 396 nitrate ions).

397 The mass balance (Table 2) and the values of apparent permeability coefficient (P<sub>app</sub>) (Table 3) were  
 398 then calculated for all NO<sub>x</sub> species. The mass balance calculated at the end of the permeability study  
 399 showed that most of the GSNO initially encapsulated or added (free) was recovered under RSNO,  
 400 nitrite ions and mostly nitrate ions species. Therefore, no NO<sub>x</sub> species were produced by cells  
 401 attesting for non-stress conditions imposed by the presence of particles.

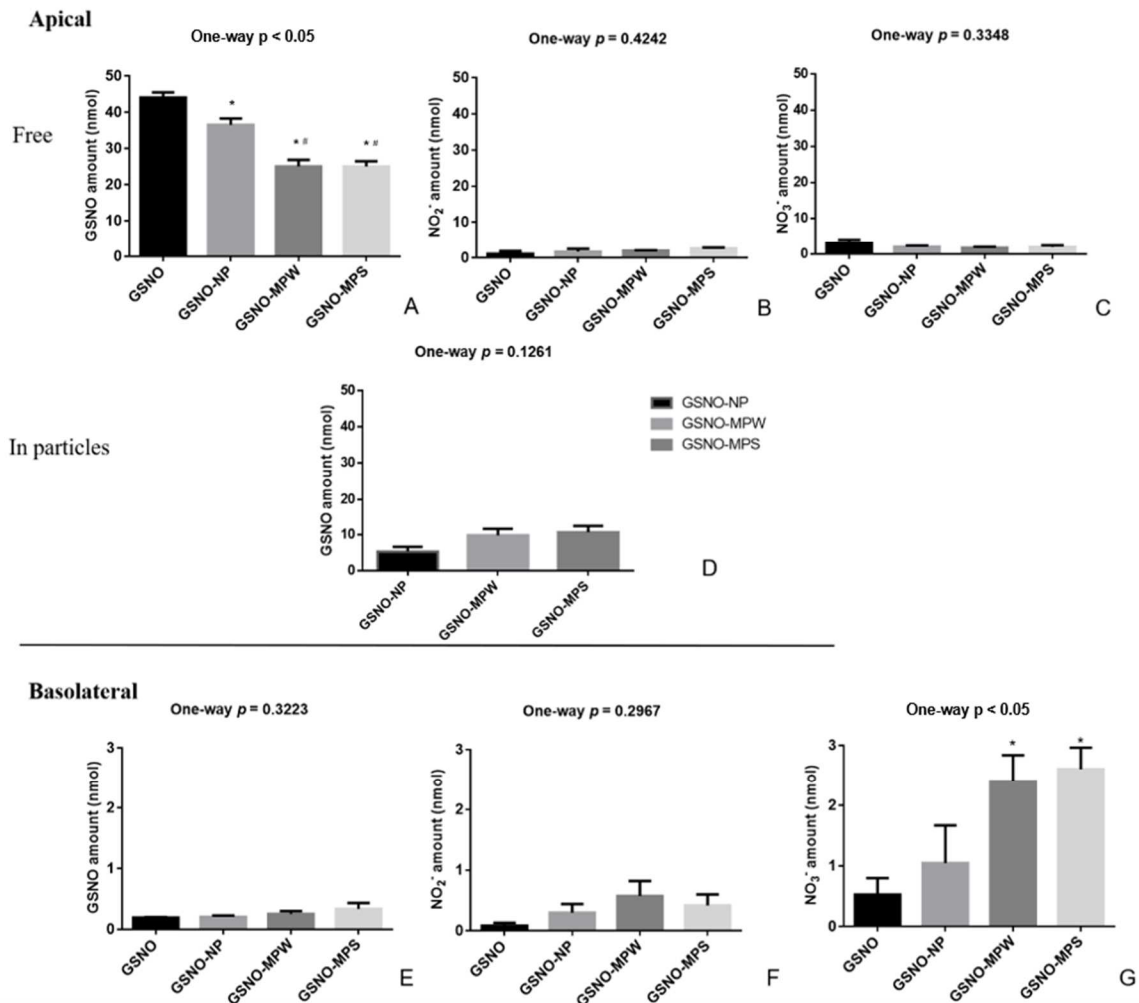
402 **Table 2. Mass balance of NO<sub>x</sub> species** for GSNO non-formulated or formulated, after 1 h of  
 403 permeability study (GSNO initial amount 50 nmol). Results are presented as mean  $\pm$  sem, n=3 in  
 404 duplicate, one-way ANOVA on each compartment (Tukey's multiple comparisons test): \*p < 0.05  
 405 *versus* GSNO.

	Amount in nmol			Total
	Apical		Basolateral	
	Free	In particles		
<b>GSNO</b>	45 $\pm$ 2 (90 $\pm$ 4%)	-	0.8 $\pm$ 0.3 (1.6 $\pm$ 0.6%)	45 $\pm$ 2 (91 $\pm$ 4%)
<b>GSNO-NP</b>	38 $\pm$ 2 (75 $\pm$ 4%)	5 $\pm$ 1 (11 $\pm$ 3%)	1.5 $\pm$ 0.8 (3 $\pm$ 2%)	44 $\pm$ 1 (89 $\pm$ 2%)
<b>GSNO-MPW</b>	32 $\pm$ 3* (62 $\pm$ 6%)	10 $\pm$ 2 (20 $\pm$ 4%)	3 $\pm$ 1 (5 $\pm$ 2%)	43 $\pm$ 1 (85 $\pm$ 2%)

<b>GSNO-MPS</b>	$30 \pm 2^*$ ( $60 \pm 5\%$ )	$11 \pm 2$ ( $21 \pm 4\%$ )	$2 \pm 1$ ( $5 \pm 2\%$ )	$43 \pm 2$ ( $86 \pm 4\%$ )
-----------------	----------------------------------	--------------------------------	------------------------------	--------------------------------

406

407 At the end of incubation, the amount of GSNO in the apical media was significantly lower for GSNO-  
 408 MPW and GSNO-MPS conditions (circa 60% of initial load) than for GSNO-NP (~75%) and free GSNO  
 409 (~90%). While around 10% of GSNO remained inside NP, almost 20% were still inside MP. This  
 410 confirms the slower release of GSNO for MP than NP, previously observed in the *in vitro* experiment,  
 411 which is even slower than in the *in vitro* release study. This can be explained by the bioadhesion  
 412 phenomenon, already observed for Eudragit RL, and the establishment of electrostatic interactions  
 413 with plasma membranes of Caco-2 cells [46]. In the meantime, both types of MP led to a drastically  
 414 higher concentration of nitrate ions (the most permeable NO species) in the basolateral side  
 415 compared to free GSNO or NP conditions (Figure 5). Despite the high local concentration of polymer  
 416 proposed in this experiment in order to deliver a quantity of RSNO that can be measured, the cells do  
 417 not endogenously produce nitrates, as shown by the mass balance (Table 2). As the same amount of  
 418 GSNO is contained in the different formulations, this result demonstrates that the same dose of  
 419 GSNO delivered by MPs, more localized with a more limited point of contact, results in greater  
 420 permeability of the naturally more permeable NO species.  
 421



422



423 **Figure 5: Quantity of GSNO, nitrite ions nitrate ions** remaining in the apical medium (A, B and C,  
 424 respectively), as well as in the basolateral medium (E, F and G, respectively), and GSNO remaining  
 425 inside the particles (D) after 1 h of permeability study (GSNO initial amount = 50 nmol in all cases).  
 426 Results are shown as means  $\pm$  sem, n=3 in duplicate, one-way ANOVA (Tukey's multiple comparisons  
 427 test): \*p < 0.05 versus GSNO and # p < 0.05 versus GSNO-NP).

428 The Papp values of each NO species are higher for the two types of GSNO-MP than for GSNO-NP or  
 429 free GSNO (Table 3). This led to a global (NOx species) Papp value at least two times higher for GSNO-  
 430 MPW and GSNO-MPS than for GSNO-NP and free GSNO. This situation is mainly driven by a higher  
 431 permeability of nitrate ions than nitrite ions and RSNO, as previously observed for non-formulated  
 432 RSNO [22]. As previously mentioned, this could be simply explained by the different distribution of  
 433 particles on the cell surface (between NP or MP). The formation of an embolus, where the dose of  
 434 GSNO is focalized on a more limited point of contact with the cell, is favorable to absorption in this *in*  
 435 *vitro* model. This phenomenon will probably be different *in vivo* because the intestinal barrier is not  
 436 limited to a cell monolayer and mucus also participates in bioadhesion phenomena.

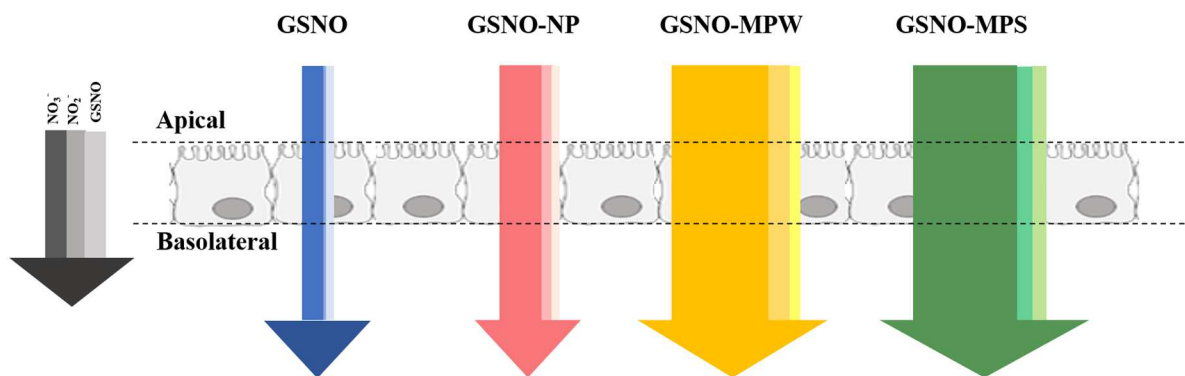
437

438 **Table 3. Values of apparent permeability coefficients (Papp)** for RSNO, nitrite ions, nitrate ions and  
 439 NOx (sum of all species) after 1 h of free GSNO, GSNO-NP or GSNO-MPs incubation. Results are  
 440 presented as mean  $\pm$  sem, n=3 in duplicate.

Treatment	Papp values ( $\times 10^{-6}$ cm.s <sup>-1</sup> )			
	RSNO	NO <sub>2</sub> <sup>-</sup>	NO <sub>3</sub> <sup>-</sup>	NOx
GSNO	0.8 $\pm$ 0.4	0.3 $\pm$ 0.2	2.0 $\pm$ 0.2	3.1 $\pm$ 0.6
GSNO-NP	0.6 $\pm$ 0.2	0.9 $\pm$ 0.3	4 $\pm$ 1	6 $\pm$ 2
GSNO-MPW	1.1 $\pm$ 0.7	1.8 $\pm$ 0.3	7 $\pm$ 1	10 $\pm$ 2
GSNO-MPS	1.1 $\pm$ 0.6	1.3 $\pm$ 0.3	8 $\pm$ 2	11 $\pm$ 2

441

442 Indeed, the three types of particles showed an improvement of the intestinal permeability of NOx  
 443 species (GSNO-MPS > GSNO-MPW > GSNO-NP) after only 1 h and without damaging the cells  
 444 monolayer (Figure 6). The Papp parameter characterizes the intestinal permeability of a drug *in*  
 445 *vitro* or *ex vivo* models. Drugs could have low permeability (Papp < 1  $\times 10^{-6}$  cm.s<sup>-1</sup>) or high  
 446 permeability ( $\geq 10 \times 10^{-6}$  cm.s<sup>-1</sup>), or be in a medium permeability class [48]. As a result, considering all  
 447 NOx species, GSNO is in the medium permeability class when administered as free GSNO or GSNO-  
 448 NP, and reaches the high permeability class using GSNO-MPs ( $\geq 10 \times 10^{-6}$  cm.s<sup>-1</sup>). This data is relevant  
 449 and the study shows that, depending on the drug delivery system used, a modulation of GSNO  
 450 absorption can be observed.



451  
 452 **Figure 6: Graphical summary of NO<sub>x</sub> species permeability for each condition** (free GSNO, GSNO-NP,  
 453 GSNO-MPW and GSNO-MPS). The width of each section of the arrows is correlated with the amounts  
 454 (from left to right) of NO<sub>3</sub><sup>-</sup>, NO<sub>2</sub><sup>-</sup> and GSNO.  
 455

456  
 457

#### 4. Conclusion

458 In this study, we overcame the challenge of getting stable and easy-to transport particles for oral  
 459 administration of GSNO. Critical parameters of the particles (i.e. size and GSNO content) were  
 460 maintained after freeze-drying, and the resulting products were stable at last one month stored at  
 461 4°C protected from oxygen. In this way, the lyophilization process has brought a very significant  
 462 improvement, since initial suspensions had to be used right after preparation. The discrepancies in  
 463 water residual content of the particles after drying indicate that MP (especially the GSNO-MPS ones)  
 464 still retain a high amount of water. This might be due to the hygroscopic properties of GSNO powder.  
 465 As GSNO is less stable in solution than in dry state, optimization of the lyophilization process could be  
 466 conducted in the future in order to reduce residual water content and therefore to improve the  
 467 stability of these GSNO-MPS. Microparticles offered a slightly slower *in vitro* release of the drug than  
 468 nanoparticles, and led to a better enhancement of NO<sub>x</sub> permeability through a model intestinal  
 469 barrier. This work confirms the importance of presenting the drug with a suitable delivery system to  
 470 the intestine. The NP and MP compared in this study could have different behaviors in *in vivo*  
 471 situations and therefore constitute tools for future GSNO oral administration in chronic conditions.

472  
 473  
 474

## References

- [1] Ignarro, L.J., 1999. Nitric oxide as a signaling molecule in the vascular system: an overview. *J. Cardiovasc. Pharmacol.* 34, 879-86. doi:10.1097/00005344-199912000-00016.
- [2] Kuhlencordt P.J., Gyurko R., Han F., Scherrer-Crosbie M., Aretz T.H., Hajjar R., Picard M.H., Huang P.L., 2001. Accelerated atherosclerosis, aortic aneurysm formation, and ischemic heart disease in apolipoprotein E/endothelial nitric oxide synthase double-knockout mice. *Circulation* 104, 448-54. doi:10.1161/hc2901.091399.
- [3] Tonelli A.R., Haserodt S., Aytekin M., Dweik R.A., 2013. Nitric oxide deficiency in pulmonary hypertension: Pathobiology and implications for therapy. *Pulm. Circ.* 3, 20-30. doi:10.4103/2045-8932.109911.
- [4] Momi S., Caracchini R, Falcinelli E, Evangelista S, Gresele P., 2014. Stimulation of platelet nitric oxide production by nebivolol prevents thrombosis. *Arterioscler .Thromb. Vasc. Biol.* 34, 820-9. doi:10.1161/ATVBAHA.114.303290.
- [5] Bienvenu L.A., Morgan J., Reichelt M.E., Delbridge L.M.D., Young M.J., 2017. Chronic in vivo nitric oxide deficiency impairs cardiac functional recovery after ischemia in female (but not male) mice. *J. Mol. Cell. Cardiol.* 112, 8-15. doi:10.1016/j.yjmcc.2017.08.012.
- [6] Hakim T.S., Sugimori K., Camporesi E.M., Anderson G., 1996. Half-life of nitric oxide in aqueous solutions with and without haemoglobin. *Physiol. Meas.* 17, 267-77. doi: 10.1088/0967-3334/17/4/004.
- [7] Zhuge Z., Paulo L.L., Jahandideh A., Brandão M.C.R., Athayde-Filho P.F., Lundberg J.O., Braga V.A., Carlström M.1., Montenegro M.F., 2017. Synthesis and characterization of a novel organic nitrate NDHP: Role of xanthine oxidoreductase-mediated nitric oxide formation. *Redox. Biol.* 13, 163-9. doi: 10.1016/j.redox.2017.05.014.
- [8] Münzel T., Daiber A., 2018. Inorganic nitrite and nitrate in cardiovascular therapy: A better alternative to organic nitrates as nitric oxide donors? *Vascul. Pharmacol.* 102, 1-10. doi: 10.1016/j.vph.2017.11.003.
- [9] Messin R., Boxho G., De Smedt J., Buntinx I.M., 1995. Acute and chronic effect of molsidomine extended release on exercise capacity in patients with stable angina, a double-blind cross-over clinical trial versus placebo. *J. Cardiovasc. Pharmacol.* 25, 558-63. Doi: 10.1097/00005344-199504000-00008.
- [10] Pereira A.C., Araújo A.V., Paulo M., Andrade F.A., Silva B.R., Vercesi J.A., da Silva R.S., Bendhack L.M., 2017. Hypotensive effect and vascular relaxation in different arteries induced by the nitric oxide donor RuBPY. *Nitric Oxide* 62, 11-6. doi: 10.1016/j.niox.2016.11.001.
- [11] Kauser N.I., Weisel M., Zhong Y.L., Lo M.M., Ali A., 2020. Calcium Dialkylamine Diazeniumdiolates: Synthesis, Stability, and Nitric Oxide Generation. *J. Org. Chem.* 85, 4807-12. doi: 10.1021/acs.joc.0c00020.
- [12] Al'Sadoni H., Ferro A., 2000. S-Nitrosothiols: a class of nitric oxide-donor drugs. *Clin. Sci. (Lond).* 98, 507-20. <https://doi.org/10.1042/cs0980507>

- [13] Perrin-Sarrado C., Zhou Y., Salgues V., Parent M., Giummelly P., Lartaud I., Gaucher C., 2020. S-Nitrosothiols as potential therapeutics to induce a mobilizable vascular store of nitric oxide to counteract endothelial dysfunction. *Biochem. Pharmacol.* 173, 113686. doi: 10.1016/j.bcp.2019.113686.
- [14] Gaucher C., Boudier A., Dahboul F., Parent M., Leroy P., 2013. S-nitrosation/denitrosation in cardiovascular pathologies: facts and concepts for the rational design of S-nitrosothiols. *Curr. Pharm. Des.* 19, 458-72. doi: 10.2174/1381612811306030458.
- [15] Liu S., Zheng H., Yu W., Ramakrishnan V., Shah S., Gonzalez L.F., Singh I., Graffagnino C., Feng W., 2020. Investigation of S-Nitrosoglutathione in stroke: A systematic review and meta-analysis of literature in pre-clinical and clinical research. *Exp. Neurol.* 328, 113262. doi: 10.1016/j.expneurol.2020.113262.
- [16] Sliskovic I., Raturi A., Mutus B., 2005. Characterization of the S-denitrosation activity of protein disulfide isomerase. *J. Biol. Chem.* 280, 8733-41. doi:10.1074/jbc.M408080200.
- [17] Stoyanovsky D.A., Tyurina Y.Y., Tyurin V.A., Anand D., Mandavia D.N., Gius D., Ivanova J., Pitt B., Billiar T.R., Kagan V.E., 2005. Thioredoxin and lipoic acid catalyze the denitrosation of low molecular weight and protein S-nitrosothiols. *J. Am. Chem. Soc.* 127, 15815-23. doi: 10.1021/ja0529135.
- [18] Barnett S.D., Buxton I.L.O., 2017. The role of S-nitrosoglutathione reductase (GSNOR) in human disease and therapy. *Crit. Rev. Biochem. Mol. Biol.* 52, 340-54. doi: 10.1080/10409238.2017.1304353.
- [19] Angeli V., Tacito A., Paolicchi A., Barsacchi R., Franzini M., Baldassini R., Vecoli C., Pompella A., Bramanti E., 2009. A kinetic study of gamma-glutamyltransferase (GGT)-mediated S-nitrosoglutathione catabolism. *Arch. Biochem. Biophys.* 481, 191-6. doi: 10.1016/j.abb.2008.10.027.
- [20] Warnecke A., Luessen P., Sandmann J., Ikic M., Rossa S., Gutzki F.M., Stichtenoth D.O., Tsikas D., 2009. Application of a stable-isotope dilution technique to study the pharmacokinetics of human <sup>15</sup>N-labelled S-nitrosoalbumin in the rat: possible mechanistic and biological implications. *J. Chromatogr. B Analyt. Technol. Biomed. Life Sci.* 877, 1375-87. doi: 10.1016/j.jchromb.2008.11.035.
- [21] Yu H., Chaimbault P., Clarot I., Chen Z., Leroy P., 2019. Labeling nitrogen species with the stable isotope <sup>15</sup>N for their measurement by separative methods coupled with mass spectrometry: A review. *Talanta* 191, 491-503. doi: 10.1016/j.talanta.2018.09.011.
- [22] Bonetti J., Zhou Y., Parent M., Clarot I., Yu H., Fries-Raeth I., Leroy P., Lartaud I., Gaucher C., 2018. Intestinal absorption of S-nitrosothiols: Permeability and transport mechanisms. *Biochem. Pharmacol.* 155, 21-31. doi: 10.1016/j.bcp.2018.06.018.
- [23] Duong H.T., Kamarudin Z.M., Erlich R.B., Li Y., Jones M.W., Kavallaris M., Boyer C., Davis T.P., 2013. Intracellular nitric oxide delivery from stable NO-polymeric nanoparticle carriers. *Chem. Commun. (Camb)*. 49, 4190-2. doi : 10.1039/c2cc37181b.
- [24] Parent M., Boudier A., Perrin J., Vigneron C., Maincent P., Violle N., Bisson J.-F., Lartaud I., Dupuis F., 2015. In Situ Microparticles Loaded with S-Nitrosoglutathione Protect from Stroke. *PLoS One* 10, e0144659. doi: 10.1371/journal.pone.0144659.
- [25] Hlaing S.P., Kim J., Lee J., Hasan N., Cao J., Naeem M., Lee E.H., Shin J.H., Jung Y., Lee B.L., Jhun B.H., Yoo J.W., 2018. S-Nitrosoglutathione loaded poly(lactic-co-glycolic acid) microparticles for

prolonged nitric oxide release and enhanced healing of methicillin-resistant *Staphylococcus aureus*-infected wounds. *Eur. J. Pharm. Biopharm.* 132, 94-102. doi: 10.1016/j.ejpb.2018.09.009.

[26] Pelegrino M.T., de Araújo D.R., Seabra A.B., 2018. S-nitrosoglutathione-containing chitosan nanoparticles dispersed in Pluronic F-127 hydrogel: Potential uses in topical applications. *J Drug Deliv Sci Technol* 43, 211-20. <https://doi.org/10.1016/j.jddst.2017.10.016>.

[27] Shah S.U., Martinho N., Socha M., Pinto Reis C., Gibaud S., 2015. Synthesis and characterization of S-nitrosoglutathione-oligosaccharide-chitosan as a nitric oxide donor. *Expert Opin. Drug Deliv.* 12, 1209-23. doi: 10.1517/17425247.2015.1028916.

[28] Shah S.U., Socha M., Fries I., Gibaud S., 2016. Synthesis of S-nitrosoglutathione-alginate for prolonged delivery of nitric oxide in intestines. *Drug Deliv.* 23, 2927-35. doi: 10.3109/10717544.2015.1122676.

[29] Shah S.U., Socha M., Sevil C., Gibaud S., 2017. Spray-dried microparticles of glutathione and S-nitrosoglutathione based on Eudragit® FS 30D polymer. *Ann. Pharm. Fr.* 75, 95-104. doi: 10.1016/j.pharma.2016.09.001

[30] Wu W., Gaucher C., Diab R., Fries I., Xiao Y.L., Hu X.M., Maincent P., Sapin-Minet A., 2015. Time lasting S-nitrosoglutathione polymeric nanoparticles delay cellular protein S-nitrosation. *Eur. J. Pharm. Biopharm.* 89, 1-8. doi: 10.1016/j.ejpb.2014.11.005.

[31] Wu W., Gaucher C., Fries I., Hu X.M., Maincent P., Sapin-Minet A., 2015b. Polymer nanocomposite particles of S-nitrosoglutathione: A suitable formulation for protection and sustained oral delivery. *Int. J. Pharm.* 495, 354-61. doi: 10.1016/j.ijpharm.2015.08.074.

[32] Wu W., Perrin-Sarrado C., Ming H., Lartaud I., Maincent P., Hu X.M., Sapin-Minet A., Gaucher C., 2016. Polymer nanocomposites enhance S-nitrosoglutathione intestinal absorption and promote the formation of releasable nitric oxide stores in rat aorta. *Nanomedicine* 12, 1795-803. doi: 10.1016/j.nano.2016.05.006.

[33] Parent M., Dahboul F., Schneider R., Clarot I., Maincent P., Leroy P., Boudier A., 2013. A complete physicochemical identity card of S-nitrosoglutathione. *Curr. Pharm. Anal.* 9, 31-42. doi: [10.2174/1573412911309010006](https://doi.org/10.2174/1573412911309010006).

[34] Pagels R.F., Prud'homme R.K., 2015. Polymeric nanoparticles and microparticles for the delivery of peptides, biologics, and soluble therapeutics. *J. Control. Release* 219, 519-35. <https://doi.org/10.1016/j.jconrel.2015.09.001>

[35] Chesa-Casalengua P., Jiang C., Bravo-Osuna I., Tucker B.A., Molina-Martinez I.T., Young M.J., Herrero-Vanrell R., 2012. Preservation of biological activity of glial cell line-derived neurotrophic factor (GDNF) after microencapsulation and sterilization by gamma irradiation. *Int. J. Pharm.* 436, 545-54. doi: 10.1016/j.ijpharm.2012.07.019

[36] He J., Li H., Liu C., Wang G., Ge L., Ma S., Huang L., Yan S., Xu X., 2015. Formulation and evaluation of poly(lactic-co-glycolic acid) microspheres loaded with an altered collagen type II peptide for the treatment of rheumatoid arthritis. *J. Microencapsul.* 32, 608-17. doi: 10.3109/02652048.2015.1065924.

[37] Liu J., Xu Y., Liu Z., Ren H., Meng Z., Liu K., Liu Z., Yong J., Wang Y., Li X., 2019. A modified hydrophobic ion-pairing complex strategy for long-term peptide delivery with high drug

- encapsulation and reduced burst release from PLGA microspheres. *Eur. J. Pharm. Biopharm.* 144, 217-29. doi: 10.1016/j.ejpb.2019.09.022
- [38] Zhang Y., Zhang Y., Guo S., Huang W., 2009. Tyrosine kinase inhibitor loaded PCL microspheres prepared by S/O/W technique using ethanol as pretreatment agent. *Int. J. Pharm.* 369, 19-23. doi: 10.1016/j.ijpharm.2008.10.032.
- [39] Han Y., Tian H., He P., Chen X., Jing X., 2009. Insulin nanoparticle preparation and encapsulation into poly(lactic-co-glycolic acid) microspheres by using an anhydrous system. *Int. J. Pharm.* 378, 159-66. doi: 10.1016/j.ijpharm.2009.05.021.
- [40] Jung J., Perrut M., 2001. Particle design using supercritical fluids: Literature and patent survey. *J. Supercrit. Fluids* 20, 179-219. [https://doi.org/10.1016/S0896-8446\(01\)00064-X](https://doi.org/10.1016/S0896-8446(01)00064-X).
- [41] Lautner G., Meyerhoff M.E., Schwendeman S.P., 2016. Biodegradable poly(lactic-co-glycolic acid) microspheres loaded with S-nitroso-N-acetyl-D-penicillamine for controlled nitric oxide delivery. *J. Control. Release* 225, 133-9. doi: 10.1016/j.jconrel.2015.12.056.
- [42] Heikal L., Starr A., Martin G.P., Nandi M., Dailey L.A., 2016. In vivo pharmacological activity and biodistribution of S-nitrosophytochelatin after intravenous and intranasal administration in mice. *Nitric Oxide* 59, 1-9. doi: 10.1016/j.niox.2016.06.006 .
- [43] Nacharaju P., Tuckman-Vernon C., Maier K.E., Chouake J., Friedman A., Cabrales P., Friedman J.M., 2012. *Nitric Oxide* 27, 150-60. doi: 10.1016/j.niox.2012.06.003.
- [44] Mordorski B., Pelgrift R., Adler B., Krausz A., Batista da Costa Neto A., Liang H., Gunther L., Clendaniel A., Harper S., Friedman J.M., Nosanchuk J.D., Nacharaju P., Friedman A.J., 2015. *Nanomedicine* 11, 283-91. doi: 10.1016/j.nano.2014.09.017 .
- [45] Yoo J.W., Lee J.S., Lee C.H., 2010. Characterization of nitric oxide-releasing microparticles for the mucosal delivery. *J. Biomed. Mater. Res. A* 92, 1233-43. doi: 10.1002/jbm.a.32434.
- [46] Paolino D. Vero A., Cosco D., Pecora T.M.G., Ciancolo S., Fresta M., Pignatello R., 2016. Improvement of oral bioavailability of curcumin upon microencapsulation with methacrylic copolymers. *Front. Pharmacol.* 7, 485. doi: 10.3389/fphar.2016.00485.
- [47] Gerloff K., Pereira D.I.A., Faria N., Boots A.W., Kolling J., Förster I., Albrecht C., Powell J.J., Schins R.P.F., 2013. Influence of simulated gastro-intestinal conditions on particle-induced cytotoxicity and interleukin-8 regulation in differentiated and undifferentiated Caco-2 cells. *Nanotoxicology* 7, 353-66. doi: 10.3109/17435390.2012.662249.
- [48] Peng Y., Yadava P., Heikkinen A.T., Parrott N., Railkar A., 2014. Applications of a 7-day Caco-2 cell model in drug discovery and development. *Eur. J. Pharm. Sci.* 56, 120-30. doi: 10.1016/j.ejps.2014.02.008.